Influence of contacts on the magnetotransport in a two-dimensional electron gas

R. Woltjer and M. J. M. de Blank
Philips Research Laboratories, NL-5600 JA Eindhoven, The Netherlands

J. J. Harris and C. T. Foxon
Philips Research Laboratories, Cross Oak Lane, Redhill, Surrey RH1 5HA, United Kingdom

J. P. André
Laboratoire d'Electronique et de Physique Appliquée, 3 avenue Descartes, 94450 Limeil–Brevannes, France
(Received 27 April 1988; revised manuscript received 8 July 1988)

The influence of electrical contacts on the magnetotransport in the quantized Hall regime is measured and calculated for various geometries in GaAs-$Al_xGa_{1-x}As$ heterostructures. The observed effects are interpreted in terms of a local resistivity tensor without taking into account the possible existence of macroscopic quantum states or localization. We approximate the experimental geometries by a network of simple rectangles with (or without) contacts. We show that this simple approach leads to a good picture of the physics behind the potential distribution. To test our approach, we measure the voltages on two multiply connected Hall bars. In special geometries with large contacts we measure a two-terminal resistance that is smaller than the Hall resistivity. Both observations can be reproduced in our calculations. Furthermore the effects of large Hall contacts in a normal Hall bar geometry are calculated and it is shown that the measured Hall resistance can be smaller than the true Hall resistance, with their difference proportional to the magnetoresistance. The dip which is often observed at the strong-field side of Hall plateaus can also be explained by the influence of (large) contacts. This shows that many of the experimental observations can be described successfully, extending our interpretation in terms of a (inhomogeneous) local resistivity tensor to real samples with metal contacts.

I. INTRODUCTION

The influence of contacts and other geometrical effects in the quantized Hall regime has been studied experimentally by many authors, e.g., Fang and Stiles,[1] Syphers and Stiles,[2] and van der Wel *et al.*[3] The results of these studies have been compared with theories by, e.g., Al'tshuler and Trunov,[4] Niu and Thouless,[5] Neudecker and Hoffmann,[6] and Rikken *et al.*[7] mainly at the magnetic fields where the Hall plateaus occur. No theory for the quantized Hall effect has, however, led to a simple algorithm from which the observable resistances can be obtained for all magnetic field strengths. Our model for the quantized Hall effect in inhomogeneous samples,[8,9] assuming the existence of a local resistivity tensor, does offer the opportunity to calculate these resistances. The model has so far been developed for a simple Hall bar geometry, and calculations have been restricted to the still simpler case of an infinitely long Hall bar geometry without contacts and with inhomogeneity over the width only.

In this paper, we will subject our approach to more stringent tests. We perform calculations for special geometries and compare them with experimental results for these geometries. The ultimate test for our description of the magnetotransport in the quantized Hall regime in terms of a local resistivity tensor would require the solution of Kirchhoff's equations in two dimensions for an inhomogeneous resistivity tensor, but this leads to serious numerical difficulties. Instead, we will extend our local resistivity description in two steps.

First, we will study geometries where the finite size of the contacts is unimportant. We divide a complex geometry into quasi-one-dimensional sections that are connected according to Kirchhoff's laws to calculate the current distribution. The magnetotransport within these sections is described by a Hall resistance and a (homogeneous) magnetoresistance per square. These resistances are obtained either from our measurements or from our model for the quantized Hall effect.[9] We will compare this description with experiments for two parallel Hall bars that are multiply connected (Sec. II). The influence of the contacts is only taken into account by the Hall voltages that are built up (due to the short circuiting of the metal) when a current flows between a metal (contact) and a semiconductor.

Second, we will study the influence of the finite size of contacts on measurable voltages. The current concentration in a pointlike corner of a contact is an approximation that disregards the penetration of part of the current over the length of a contact. In Sec. III we discuss this additional effect and solve Kirchhoff's equations for the case of a stripe of semiconductor (with homogeneous resistivity tensor) parallel to a metal contact. We will pay attention to the effects of a finite contact resistance and of inhomogeneities in the two-dimensional electron system.

Section IV deals with experiments on GaAs-$Al_xGa_{1-x}As$ heterostructures in special geometries with

large contacts, carried out to test the combination of the approaches in Secs. II and III. For our calculations we describe the geometry of a sample by a network of simple rectangles (with an uniform resistivity), some of them with metal contacts along them. Because interesting effects occur at weaker magnetic field strengths, where we do not have an accurate resistivity tensor for our model, we used the measured Hall resistance and magnetoresistance (per square) as input in our calculations of the potential distribution. We will show that, and explain why, the two-terminal resistance in certain geometries with large contacts can be smaller (or larger) than the Hall resistivity. Furthermore, we will discuss the influence of large Hall contacts on magnetotransport measurements in a standard Hall bar geometry.

In Sec. V we compare two nearly identical geometries where the current must choose between two parts of the sample. In the first sample this choice is made in the metal contacts, whereas in the second geometry the choice is made in the two-dimensional electron system itself. The difference in behavior can be explained qualitatively by solving Kirchhoff's equations, again taking into account the Hall voltages at the metal-semiconductor interfaces.

Our use of a local resistivity tensor is worth mentioning, because some theories describe the quantized Hall effect in terms of macroscopic quantum states that extend over a sample. Other theories are based on localized states that exclude certain regions in a sample from participation in the current transport. Our results will show that, in spite of these nonlocal effects, a local description of the resistivity can be useful.

For all the calculations in this paper it is important to realize that in our local description the current distribution within the two-dimensional electron system is (in a good approximation) determined by the local magnetoresistivity only.[9] For small currents, the distribution of the Hall voltage over the sample has no influence on the current distribution within the semiconductor when the Hall resistivity shows no appreciable variations.

These geometry-dependent experiments can only lead to meaningful results in samples of excellent quality. The material has to be fairly homogeneous and the electrical contacts must be Ohmic with low resistances. It is worth noting here that the same experiments in worse materials can possibly lead to quite different results. All our experiments were done in high-quality samples with good contacts and expected symmetries were checked by changing the direction of the magnetic field or the current to see whether the observed effects are due to the intended geometrical effects, inhomogeneity, or uninteresting imperfections of the samples.

II. DIVIDING COMPLICATED GEOMETRIES IN SIMPLE SECTIONS

We extend the description of a Hall bar in terms of an infinite one-dimensional stripe without contacts[9] to a more realistic one. The geometry of a standard Hall bar geometry with two pairs of Hall contacts is given in the upper part of Fig. 1. We consider the two-dimensional

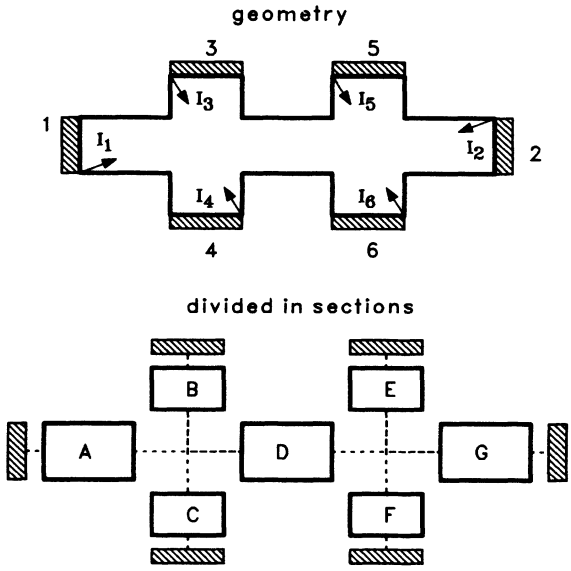

FIG. 1. Standard Hall bar geometry with two pairs of Hall contacts. The corners where (most of) the current enters the metal contacts, due to the magnetic field, are denoted by the numbered arrows in the Hall bar. To simplify the calculations we split this geometry in seven semiconductor sections and six-metal contacts which are connected (dotted lines) according to Kirchhoff's laws, as sketched below.

electron system as a proper connection of seven one-dimensional parts, as schematically given at the bottom of the same figure, in which we describe the electrical transport by their Hall resistance and their magnetoresistance per square. Where semiconductor sections are connected we obey Kirchhoff's laws by requiring current conservation and equal potentials. Note that for small currents only ρ_{xx} determines the current distribution, making the Hall effect unimportant at the interface between two semiconductor sections which have equal ρ_{xy}. The Hall voltages that are generated at the boundary between a metal contact and the two-dimensional electron system (in the corners where the arrows denote the currents) are taken into account, neglecting the effects of the finite sizes of the contacts.

We calculate the magnetotransport starting from the magnetoresistance per square $R_\square \equiv R_{xx}^\square$ and the Hall resistance $R_H \equiv R_{xy}$. In the figure we have indicated in which corner of the contacts most of the current flows due to the magnetic field and the definitions of the currents. The symbols $N_\square$ with their superscripts denote the number of squares of a section of the sample, with the superscript referring to the section. The number of squares is the ratio of the length (parallel to the current) over the width (perpendicular to the current) of a rectangular section. As an example, we consider how $V_{3,2}$ is obtained. Between contact 2 and contact 3 we have a Hall voltage, $-I_2 R_H$, generated by the current between contact 2 and the semiconductor and a Hall voltage, $-I_5 R_H$, generated by the current passing through contact 5. The magnetoresistance causes a voltage drop $-I_2 N_{\square G} R_\square$ in Sec. G $(I_1+I_3+I_4)N_{\square D}R_\square$ in Sec. D,

and $I_3 N_{\square B} R_\square$ in Sec. B. Comparable reasoning leads to five voltages as a function of the six currents,

$$V_{1,2}=(I_1+I_4+I_6)R_H-I_2N_{\square G}R_\square +(I_1+I_3+I_4)N_{\square D}R_\square+I_1N_{\square A}R_\square\ , \quad (1)$$

$$V_{3,2}=-(I_2+I_5)R_H-I_2N_{\square G}R_\square +(I_1+I_3+I_4)N_{\square D}R_\square+I_3N_{\square B}R_\square\ , \quad (2)$$

$$V_{4,2}=(I_4+I_6)R_H-I_2N_{\square G}R_\square +(I_1+I_3+I_4)N_{\square D}R_\square+I_4N_{\square C}R_\square\ , \quad (3)$$

$$V_{5,2}=-I_2R_H-I_2N_{\square G}R_\square+I_5N_{\square E}R_\square\ , \quad (4)$$

$$V_{6,2}=I_6R_H-I_2N_{\square G}R_\square+I_6N_{\square F}R_\square\ . \quad (5)$$

Use of $I_1+I_2+I_3+I_4+I_5+I_6=0$ results in five voltages and five independent currents for the Hall bar with six contacts. We will use this six-pole description of a Hall bar to calculate the voltages on the contacts of two Hall bars electrically connected in parallel and compare our results with experimental data on this geometry. The experimental situation is schematically given in Fig. 2, where the contacts (shaded) on both Hall bars are numbered. Both Hall bar geometries are made on standard GaAs-$Al_xGa_{1-x}As$ heterostructures. For all the experiments described in this section, the current contacts were connected by metal wires as shown in the figure by the solid lines. In some experiments the Hall contacts of both Hall bars were also connected. As an example we have drawn the links between these contacts with dotted lines for the case that all Hall contacts are connected with their corresponding contact on the other Hall bar. The mean electron densities for sample A and sample B are 4.17×10^{15} m^{-2} and 4.84×10^{15} m^{-2}, respectively. The mobilities are 13.1 m^2/Vs and 9.63 m^2/Vs, respectively. The temperature is kept constant at 2.2 K during all experiments and the current I_0 is 1 μA.

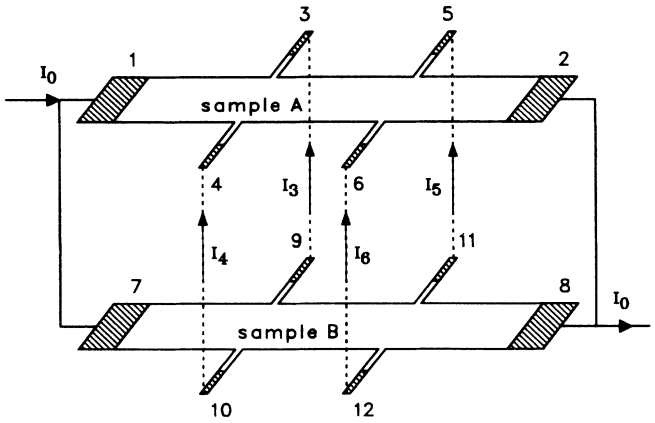

FIG. 2. Two Hall bars connected electrically in parallel by metal wires. The metal contacts are shaded. The current contacts (1, 2, 7, and 8) are connected in pairs for all the experiments in this section. The Hall contacts (3, 4 5, 6, 9, 10, 11, and 12) can also be connected as shown by the dotted lines for the case that all corresponding contacts are connected.

We calculate the voltages on the contacts with respect to ground (contact 2) by using the six-pole equations. The magnetoresistance per square $R_\square$ and the Hall resistance R_H are calculated with the inhomogeneity model,[9] using the experimentally determined parameters for the samples and including an inhomogeneity of 2.6%. The number of squares of each section is determined from the geometry of the samples used in the experiments. We have $N_{\square A}=N_{\square G}=(350\ \mu m)/(150\ \mu m)\approx2.3$, $N_{\square D}=(400/\mu m)/(150/\mu m)\approx2.7$ and $N_{\square B}=N_{\square C}=N_{\square E}=N_{\square F}=(80\ \mu m)/(20\ \mu m)=4$ in both Hall bars.

Figures 3(a) and 3(b) give the results of experiments and calculations, respectively, for the case of nonconnected Hall contacts, making $I_3=I_4=I_5=I_6=0$. Even though R_H and $R_\square$ used for these calculations are only approximate, we clearly see that the calculated voltages show features that also show up in the experimental observations: The Hall voltages oscillate around the classical Hall voltages with a minimum amplitude around 1.3 T and the "parallel" voltages have a double peak around 3.8 T.

Figures 4(a) and 4(b) give the results of experiments

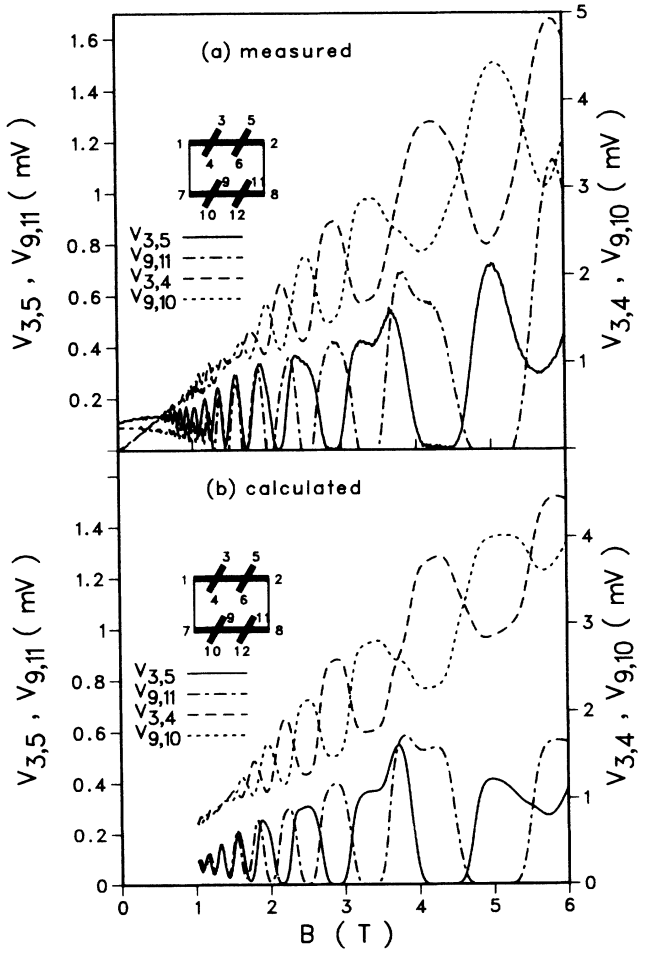

FIG. 3. (a) Measured and (b) calculated voltages between Hall probes for two parallel Hall bars. No connections between the Hall probes exist in this situation.

and calculations, respectively, for the case of two connected Hall contacts: $V_4=V_{10}$ and $V_6=V_{12}$. In this case $I_3=I_5=0$. The extra connections on one side of the Hall bars lead to a peculiar oscillatory behavior of the voltage on that side with a minimum amplitude around 3 T. This feature as well as the different Hall voltages are clearly reproduced in our calculated results. The extra connections on one side do not have any important influence on the voltages on the other side.

Figures 5(a) and 5(b) give the results of experiments and calculations, respectively, for the case of four extra connections $V_3=V_9$, $V_4=V_{10}$, $V_5=V_{11}$, and $V_6=V_{12}$. No constrictions on the currents arise in this case. Only two different voltages exist in our calculations for symmetry reasons. Due to imperfections in the samples the experimentally observed voltages differ slightly from each other, but they all show the peculiar oscillations in the parallel voltages that are described for the previous case. The Hall voltage approaches the classical (linear) B dependence due to the extra connections. Apart from imperfections in the sample, which are not taken into account in our calculations, we have no explanation for the fact that the oscillations in the Hall voltages are more pronounced in the experiments than in the calculations.

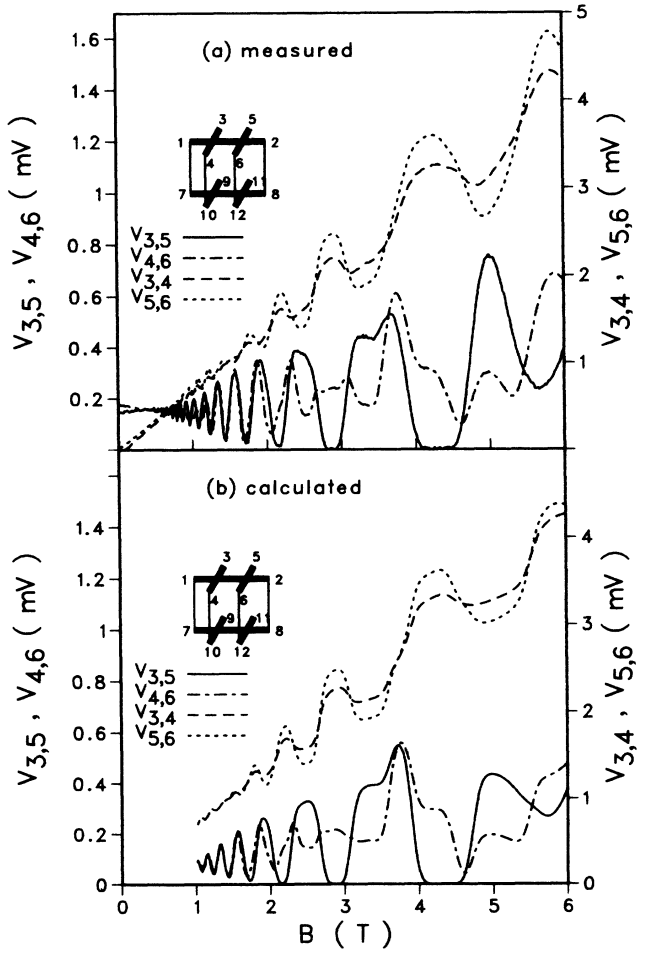

FIG. 4. (a) Measured and (b) calculated voltages between Hall probes for two parallel Hall bars. Two connections exist between Hall probes 4 and 10 as well as between 6 and 12.

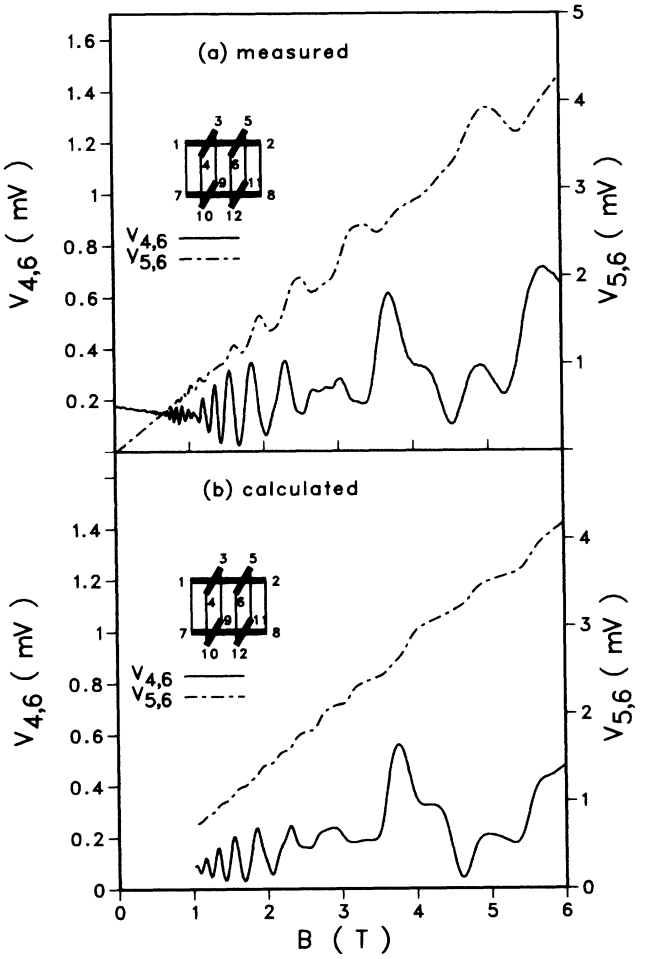

FIG. 5. (a) Measured and (b) calculated voltages between Hall probes for two parallel Hall bars. Four connections exist between Hall probes 3 and 9, 4 and 10, 5 and 11, 6 and 12, respectively.

The results show that our description of the magnetotransport by a local resistivity tensor, taking into account the Hall voltages that are built up when current enters metal contact corners, leads to reasonable results for the measurable potentials even in complicated geometries. In addition to the Hall voltages caused by a current which enters a (small) contact (for $\rho_{xx}<\rho_{xy}$ in the semiconductor), we can have an important additional effect when (for $\rho_{xx}\neq 0$ in the semiconductor) a current flows along a large contact. This will be discussed in the next section.

III. CURRENT DISTRIBUTION NEAR CONTACTS

Until now we have disregarded the influence of the finite contact size on the magnetotransport measurements. In Sec. IV we will investigate the influence of large contacts in experiments, but first we will analyze what we would expect when the magnetotransport in the vicinity of a metal contact is described in terms of a local resistivity tensor. In Fig. 6 we have sketched a two-dimensional electron system between a metal contact

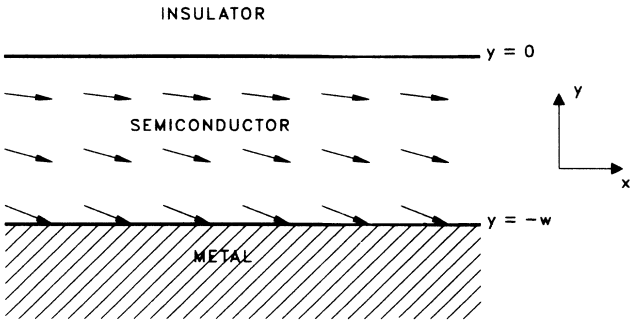

FIG. 6. Details of a metal-semiconductor interface. The x and y directions are given on the right. The metal-semiconductor interface is an equipotential line. A nonzero ρ_{xx} inside the semiconductor makes the current across the equipotential lines and flow into the metal. The arrows indicate the directions of the current flow for the magnetic field in the positive z direction.

($y<-w$) and an insulator ($y>0$). We denote physical quantities in the metal by a superscript m to distinguish them from quantities in the semiconductor without superscripts. Inside the metal we take $\rho_{xx}^m=0$ and $\rho_{xy}^m=0$, which is a reasonable approximation as we will show later. In this ideal metal no potential differences can exist, leading to $E_x=0$ at the metal-semiconductor interface. The Hall angle $\theta_H=\arctan(\rho_{xy}/\rho_{xx})$ is the angle between the electric field and the current. For $\rho_{xx}\neq 0$ the current crosses equipotential lines. Thus part of the current flowing along the metal contact leaves the two-dimensional electron system and penetrates into the metal (for one direction of the magnetic field).

We describe this penetration for the simple case of a homogeneous sample with ρ independent of the spatial coordinates. Kirchhoff's laws reduce to

$$\mathrm{div}\mathbf{J}=\frac{\partial J_x}{\partial x}+\frac{\partial J_y}{\partial y}=0$$

and

$$(\mathrm{curl}\mathbf{E})_z=\rho_{xx}\left[\frac{\partial J_y}{\partial x}-\frac{\partial J_x}{\partial y}\right]=0\ . \tag{6}$$

Of course, $J_y(x,0)=0$ at the upper boundary $y=0$. A stationary current distribution for $x\to\infty$ leads, in combination with the translation symmetry of the geometry in the x direction, to $J_y(\infty,y)=0$. This results in

$$J_x(x,y)=J_0e^{-x/\alpha}\cos(y/\alpha)+J_\infty$$

and

$$J_y(x,y)=J_0e^{-x/\alpha}\sin(y/\alpha)\ . \tag{7}$$

The continuity of $E_x(x,-w)$ at the metal-semiconductor interface determines the length α, because $E_x=\rho_{xx}J_x+\rho_{xy}J_y=0$ results in

$$\rho_{xy}+\rho_{xx}\left[\frac{J_x(x,-w)}{J_y(x,-w)}\right]=\rho_{xy}-\rho_{xx}\cot(w/\alpha)=0\ , \tag{8}$$

where $J_\infty=0$ follows from the continuity of $E_x(\infty,-w)$. Note that α is typically larger than the semiconductor width w in the quantized Hall regime, because $\rho_{xx}<\rho_{xy}$. The current I flowing in the positive x direction through the semiconductor is given by

$$I=\int_{-w}^{0}J_x\,dy=\alpha J_0e^{-x/\alpha}\sin(w/\alpha)\ . \tag{9}$$

For the homogeneous case we can replace the components of the local resistivity tensor by the measurable resistances: $\rho_{xx}\to R_\square$ and $\rho_{xy}\to R_H$. By combining (8) and (9), introducing a reduced unit of length $N_\square=x/w$ (the number of squares) and denoting $\alpha J_0\sin(w/\alpha)=I_0$ we finally obtain

$$I(N_\square)=I_0\exp\left[-N_\square\arctan\frac{R_\square}{R_H}\right]$$
$$\approx I_0\exp\left[-N_\square\frac{R_\square}{R_H}\right]\approx I_0\left[1-N_\square\frac{R_\square}{R_H}\right]\ . \tag{10}$$

A current flowing in a homogeneous two-dimensional electron system along a metal contact will indeed partially flow into the contact when the magnetoresistivity in the semiconductor is finite; the current in the two-dimensional electron system will decrease exponentially with distance, when passing the contact. Our treatment so far contains two simplifying assumptions. We have dealt with an ideal metal and a homogeneous semiconductor. We will first discuss the influence of these assumptions before we study such effects in experiments with large contacts in Sec. IV.

We assumed an ideal metal for the contacts; $\rho_{xx}^m=0$ and $\rho_{xy}^m=0$. Although $\rho_{xy}^m<\rho_{xy}$ due to the higher electron density in the metal, the resistivity per square in the metal ρ_{xx}^m can be larger than ρ_{xx}, especially for magnetic fields that result in integer filling factor in the semiconductor. We will give the results for a metal contact between $y=-w$ and $y=-2w$ in Fig. 6. We can find a solution of (6) in the metal that is comparable to (7). Continuity of $E_x(x,-w)$ leads in this case to

$$\rho_{xy}+\rho_{xx}\left[\frac{J_x(x,-w)}{J_y(x,-w)}\right]=\rho_{xy}^m+\rho_{xx}^m\left[\frac{J_x^m(x,-w)}{J_y^m(x,-w)}\right]\ . \tag{11}$$

Since $\mathrm{div}\mathbf{J}=0$ implies that J_y is continuous over the metal-semiconductor interface, the length α is the same in metal and semiconductor. From $J_y(\infty,-w)=0$ we see that $\rho_{xx}J_\infty=\rho_{xx}^mJ_\infty^m$. This leads to

$$\rho_{xy}-\rho_{xx}\cot(w/\alpha)=\rho_{xy}^m+\rho_{xx}^m\cot(w/\alpha)\ . \tag{12}$$

For the case that, at $x=0$, no current flows in the x direction inside the metal and $I=I_0$ we finally obtain

$$I(N_\square)=\frac{R_\square I_0}{R_\square+R_\square^m}\exp\left[-N_\square\arctan\left[\frac{R_\square+R_\square^m}{R_H-R_H^m}\right]\right]$$
$$+\frac{R_\square^mI_0}{R_\square+R_\square^m}\approx I_0\left[1-N_\square\frac{R_\square}{R_H-R_H^m}\right]\ . \tag{13}$$

Comparison of (10) and (13) clearly shows that the influence of a good metal is negligible already at

moderate magnetic field strengths. Even at an integer filling factor the resistance of the metal is not important for a current flowing along a contact.

The effects of a current leaving a two-dimensional electron system in the corner of a (current carrying) metal contact were studied for the two-terminal resistance near the integer filling factor by Rikken *et al.*[7] and found to be at the ppm level. Thus the assumption of an ideal metal will not severely disturb our results.

The second simplification in our calculations is the assumption that the local resistivity tensor is independent of the spatial coordinates. This assumption is in apparent contradiction with our model for the quantized Hall effect.[9] In the quasi-one-dimensional approximation, we assumed that ρ changes over the width (y direction) only. In this case no simple solution exists, but taking ρ_{xy} independent of y (variations in the electron density are small) and taking $\rho_{xx}(y)$, we obtain an exponential behavior again. This is due to the fact that the current leaving the semiconductor stripe is in that case proportional to the current passing through the stripe.

For a two-dimensional inhomogeneity we may have corrections to the exponential behavior, but with random inhomogeneities there is no reason why the (qualitative) behavior would be significantly different. We describe the magnetotransport by an effective resistivity tensor that is a proper average over the inhomogeneous local resistivity tensor when a sample contains no large-scale inhomogeneities like gradients or large regions with different mean electron densities. This is the way in which we will look at the calculations in Secs. IV and V.

IV. INTERPRETATION OF EXPERIMENTS WITH LARGE CONTACTS

We have performed experiments on GaAs-$Al_xGa_{1-x}As$ heterostructures with special geometries to test the combination of approaches described in Secs. II and III. A disputable assumption is the use of a homogeneous description that enables us to define $R_\square$ and to use the number of squares to describe geometries. We will describe our geometries as a series connection of rectangles without contacts and rectangles with contacts, described according to Sec. III. These simplifications make it easier to get insight into the physics of two-dimensional current transport in the neighborhood of a metal contact.

We will first describe the results obtained with the "open square" geometry as sketched in Fig. 7. The magnetic field is perpendicular to the sample and the current $I_0=1$ μA is flowing from contact 1 to contact 3. The voltages measured between contacts 4 and 2 as well as between 2 and 7 are shown in Fig. 8(a) for one direction of the magnetic field. Both curves show the expected behavior for a magnetoresistance measurement. The main difference is in the amplitude of the two signals. The voltage measured between 7 and 2 is nearly three times larger above 0.3 T. It is clear that in a symmetric geometry this can only occur due to the presence of the magnetic field. Reversion of the direction of the magnetic field leads to the expected interchange in behavior of the two voltages, $V_{4,2}$ and $V_{2,7}$. Reversion of the direction of the current through the sample only changes the signs of the voltages, showing that our observations are not due to unintentional asymmetries in the geometry of the sample.

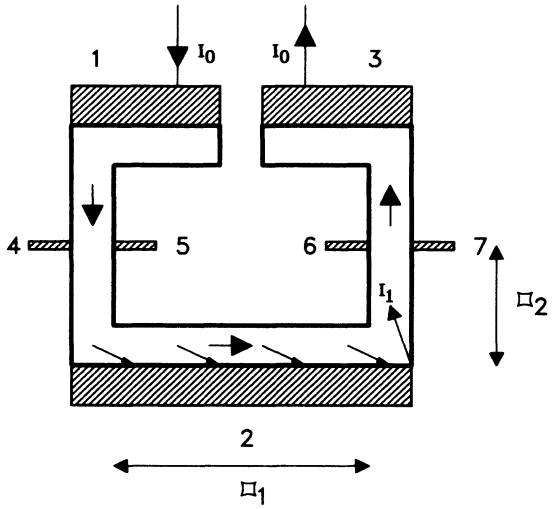

FIG. 7. The "open square" geometry used in experiments to measure the influence of metal contacts on the potential distribution. The current I_0 is flowing from contact 1 to 3. The direction of the current flow, for one direction of the magnetic field, is indicated by the arrows. The current I_1 enters contact 2 over its length and leaves it in its right corner.

We describe the sample by a series connection of three sections; two sections of semiconductors (lengths $2N_{\square_2}$) connected by one section of semiconductors parallel to a metal (length $N_{\square_1}$). We obtain the following equations:

$$\frac{V_{4,2}}{I_0}=N_{\square_2}R_\square\ , \tag{14}$$

$$\frac{V_{2,7}}{I_0}=R_H[1-\exp(-N_{\square_1}R_\square/R_H)]+N_{\square_2}R_\square$$

$$\approx(N_{\square_1}+N_{\square_2})R_\square \tag{15}$$

The first contribution in the right-hand side of (15) is due to the current $I_1=I_0-I(N_{\square_1})$ that enters contact 2 over its full length and leaves that contact in the right corner. For $R_H>N_{\square_1}R_\square$, we see that $V_{4,2}$ and $V_{2,7}$ both exhibit a magnetoresistance type of behavior. From the geometry used in the experiments we determined $N_{\square_1}\approx(600\ \mu\text{m})/(100\ \mu\text{m})=6$ and $N_{\square_2}\approx(300\ \mu\text{m})/(100\ \mu\text{m})=3$ and find a factor $(N_{\square_1}+N_{\square_2})/N_{\square_2}\approx3$ between both voltages, in accordance with our observations.

The resistivity tensor, used in our model for the quantized Hall effect, is only applicable for stronger magnetic fields, making detailed comparison with experiments in weaker magnetic fields ($B<1$ T), where the exponential dependence is important, impossible. For comparison of our calculations with the experiments we use the measured magnetoresistance per square $R_\square=V_{4,2}/(3I_{1,3})$

and Hall resistance $R_H = V_{5,4}/I_{1,3}$, respectively. The results of these calculations are shown in Fig. 8(b) and show convincing agreement with experimental results. In the calculations it is obvious that the voltages $V_{2,7}$ and $V_{4,2}$ interchange in behavior for the other polarity of the magnetic field. In weaker magnetic fields we expect to see the influence of the exponential factor in (15), resulting in a lower value for $V_{2,7}$. In Fig. 8 the expected decrease of $V_{2,7}$ is clearly visible below 0.3 T, whereas $V_{4,2}$ is nearly constant. The physical picture for this smaller resistance in weaker magnetic fields is that all current will enter contact 2 (low resistance) at the left-hand side and leave it at the right-hand side, thus avoiding the magnetoresistance in the semiconductor parallel to the metal contact.

Another geometry that gives peculiar results is the "open Corbino" geometry shown in the inset of Fig. 9. This is essentially a normal Corbino geometry with a small sector of the electron system cut out to prevent circulating currents. By conformal mapping it can be shown that this geometry is comparable with a short Hall bar geometry as described by Beer.[10] The two-terminal resistance between the inner (radius 200 μm) and the outer (radius 700 μm) contacts is given in the same figure. At the magnetic field strengths where the magnetoresistance is zero we observe the quantized Hall effect. For comparison we give the Hall resistance measured in a Hall bar geometry of the same material. Between the plateaus the two-terminal resistance is smaller than the Hall resistance and their difference is proportional to the magnetoresistance. This behavior is very different from the observations in a long Hall bar geometry, where the two-terminal resistance is the sum of Hall resistance and magnetoresistance.[1] The important difference between the long Hall bar and the open Corbino (or the short Hall bar) is that in the last case the current flows along a metal contact over a large distance, where part of the current leaves the semiconductor when $\rho_{xx} \neq 0$. This leads to a negative contribution to the two-terminal resistance R_{io} because the Hall voltage that is built up in the corner of the contacts is generated by a smaller current according to (10),

$$R_{io} = R_H \exp(-N_{\square_1} R_\square / R_H) + N_{\square_2} R_\square \approx R_H + (N_{\square_2} - N_{\square_1}) R_\square \, . \quad (16)$$

Here $N_{\square_1}$ is the length over which the current flows parallel to a contact and $N_{\square_2}$ is the remaining length of the current path.

We finish this paragraph by a calculation of the effects of large Hall contacts on the standard magnetotransport measurements, using the geometry given in Fig. 10. This is a standard Hall bar geometry with two large Hall contacts. The direction of the current flow for one direction

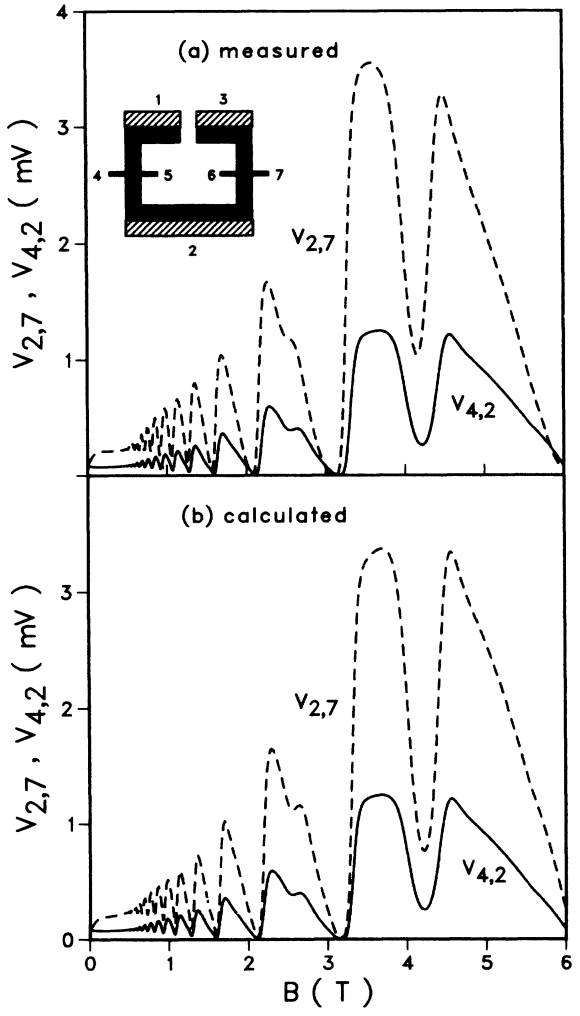

FIG. 8. (a) Measured and (b) calculated voltages between two contacts of the open square geometry sketched in Fig. 7. The current is $I_0 = 1$ μA between contacts 1 and 3. The calculations use measured R_H and $R_\square$.

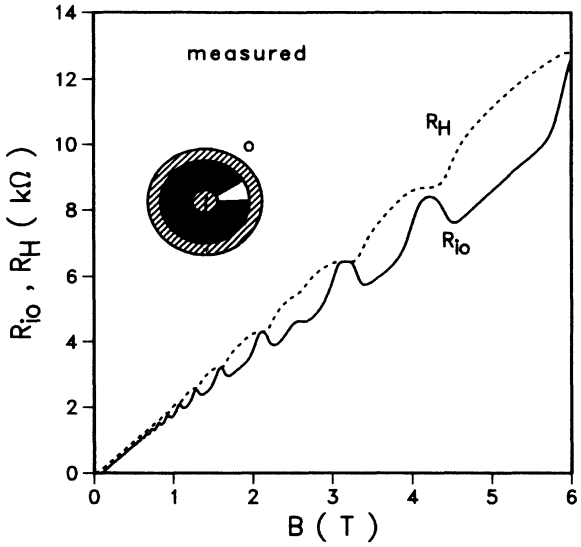

FIG. 9. Two-terminal resistance R_{io} between the two contacts of the "open Corbino" geometry sketched in the inset. For comparison we give the Hall resistance R_H as measured in a Hall bar geometry made of the same material. The two-terminal resistance is smaller than the Hall resistance, due to the large contacts.

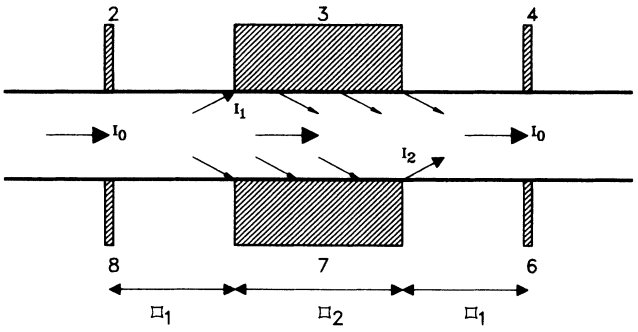

FIG. 10. Hall bar geometry with two large Hall contacts in the middle. The direction of the current flow for one direction of the magnetic field is indicated by arrows. The total current flowing from left to right is I_0. The current passing through contact 3 is I_1 and that passing through contact 7 is I_2.

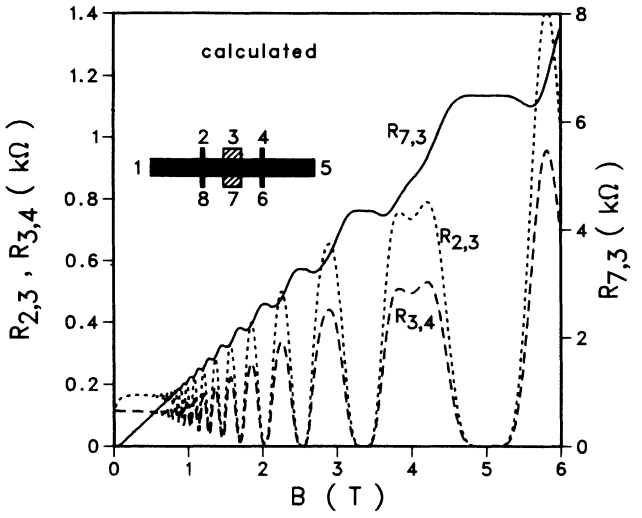

FIG. 11. Calculated Hall and magnetoresistance for the Hall bar geometry with two large Hall contacts, as given in Fig. 10. The Hall voltage between 3 and 7 is smaller than the true Hall voltage between 2 and 8 owing to the effects of the large contacts. The calculations start with measured R_H and $R_\square$.

of the magnetic field is indicated by arrows in the Hall bar to show what contributions we can expect. The current entering contact 3 in the left corner is called I_1 and that leaving contact 7 in the right corner is called I_2. The resistances $R_{3,7}$ $R_{2,3}$, and $R_{3,4}$ are given by

$$R_{3,7}=\frac{R_H(I_0-I_1)}{I_0}$$

$$=R_H\exp(-N_{\square_2}R_\square/R_H)\approx R_H-N_{\square_2}R_\square\ , \tag{17}$$

$$R_{2,3}=\frac{R_HI_2+N_{\square_1}R_\square I_0}{I_0}=R_H[1-\exp(-N_{\square_1}R_\square/R_H)]$$

$$+N_{\square_1}R_\square\approx(N_{\square_1}+N_{\square_2})R_\square\ , \tag{18}$$

$$R_{3,4}=\frac{N_{\square_1}R_\square I_0}{I_0}=N_{\square_1}R_\square\ . \tag{19}$$

From these equations we learn that large contacts will reduce the measured Hall resistance $R_{3,7}$, independent of the direction of the magnetic field, as observed by Cage *et al.*[11] The resistance between two contacts $R_{2,3}$ divided by the number of squares between the contacts can be large [by a factor of $(1+N_{\square_2}/N_{\square_1})$ in this case] than the true magnetoresistance per square. We have not performed experiments to test these calculations, but we have calculated the resistances starting from measured $R_\square$ and R_H to show the effects. The results of these calculations are presented in Fig. 11 for $N_{\square_1}=1$, $N_{\square_2}=\frac{1}{2}$. We clearly see a dip at the strong-magnetic field side of the Hall plateaus, as observed, e.g., by Cage *et al.*[11] due to the large contacts. This dip is independent of the direction of the magnetic field. A (partial) dependence on the direction of the magnetic field can be explained by a component of the current flowing in the direction of the Hall contacts, as suggested earlier.[8] From these calculations we can conclude that a Hall bar geometry which is intended to be used for high-precision measurements on the quantized Hall effect should have small Hall contacts, or it must have long and narrow side arms where hardly any currents flows, as sketched for our standard Hall bar geometries in Fig. 2.

V. CURRENT DISTRIBUTION DETERMINED IN METAL OR SEMICONDUCTOR

In this section we will study the difference in the distribution of the current between two square geometries. The "open square" geometry with short-circuited current contacts and the "closed square" geometry are both sketched in the insets of Fig. 12. In both cases the current is passing between contact 1 and 2 through a geometry with two branches over which the Hall voltage can be measured between the contact pairs 4,5 and 6,7. In the open square geometry the current must choose between the branches when it is in the metal, thus influenced by the Hall voltages that are built up where the current enters the contacts. In the closed square geometry this choice is made in the two corners of the semiconductor where the current flows, thus influenced by the magnetoresistance in the semiconductor only.

The experimental results for $I_0=1$ μA between contacts 1 and 2 are given in Fig. 12. In both cases the sum of $V_{4,5}$ and $V_{6,7}$ is the quantized Hall voltage as expected. The main difference is the distribution of the Hall voltage over the two branches, which is asymmetric in the open square geometry, whereas it is nearly symmetric in the closed square geometry (apart from the magnetic field strengths where the plateaus in the sum of the Hall voltages occur). When the direction of the magnetic field is changed in the open square geometry the asymmetric Hall voltages are interchanged, confirming that the asymmetry is not due to an unintentional asymmetry in the

geometry. When the magnetic field changes sign in the closed square geometry the Hall voltages only change signs, suggesting again that the effects are not caused by the geometry but, for instance, by the inhomogeneity of the electron density. The observations in the ring geometry that are analyzed extensively[9] are very comparable to the closed square geometry in that sense.

The distribution of the current over the open square geometry can be calculated by solving Kirchhoff's equations for our simple approach describing the influence of contacts by the model described in Sec. 3. The voltages on the contacts 1 and 3 with respect to contact 2 are given by

$$V_{1,2}=R_H I_1+2N_{\square_2}R_\square I_1 \ , \tag{20}$$

$$V_{3,2}=R_H[I_1\exp(-N_{\square_1}R_\square/R_H)+I_2]+2N_{\square_2}R_\square I_2 \ , \tag{21}$$

where I_1 flows in the left branch of the square and I_2 in the right branch. The connection of contacts 1 and 3 means that both voltages are equal, resulting in a value for I_1 and I_2 that enables us to calculate the two Hall voltages

$$V_{4,5}=R_H I_1=\frac{(R_H+2N_{\square_2}R_\square)R_H I_0}{R_H[2-\exp(-N_{\square_1}R_\square/R_H)]+4N_{\square_2}R_\square}$$

$$\approx\frac{(R_H+2N_{\square_2}R_\square)R_H I_0}{R_H+(N_{\square_1}+4N_{\square_2}R_\square} \ , \tag{22}$$

$$V_{6,7}=R_H I_2$$

$$=\frac{\{R_H[1-\exp(-N_{\square_1}R_\square/R_H)]+2N_{\square_2}R_\square\}R_H I_0}{R_H[2-\exp(-N_{\square_1}R_\square/R_H)]+4N_{\square_2}R_\square}$$

$$\approx\frac{(N_{\square_1}+2N_{\square_2})R_\square R_H I_0}{R_H+(N_{\square_1}+4N_{\square_2})R_\square} \ . \tag{23}$$

The asymmetry between both Hall voltages is clear from these equations. For $R_\square \ll R_H$, the voltages $V_{4,5}$ and $V_{6,7}$ correspond to a Hall resistance and a magnetoresistance, respectively.

Experimentally determined $R_\square$ and R_H have been used (see Sec. IV for the arguments). The calculated voltages are given in Fig. 13. We clearly see the characteristic difference between the two, but the quantitative similarity with Fig. 12(a) is not complete. This is probably due to the simplifications in our calculations; we started from a homogeneous resistivity tensor and approximated the sample by a network of rectangles. When the resistivity has systematic inhomogeneities we cannot use the number of squares, but we should solve the complete two-dimensional problem for the distribution of the resistivity

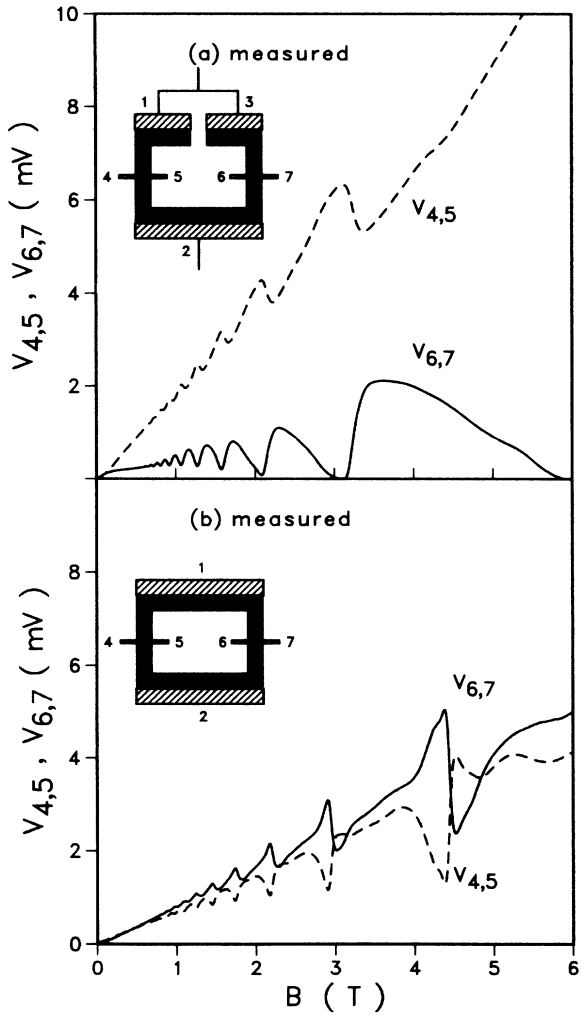

FIG. 12. Measured Hall voltages on two geometries for a current flowing between contact 1 and 2. We have (a) the "open square" geometry with contact 1 and 3 short-circuited and (b) the "closed square" geometry. Both geometries are given in the insets of the figures.

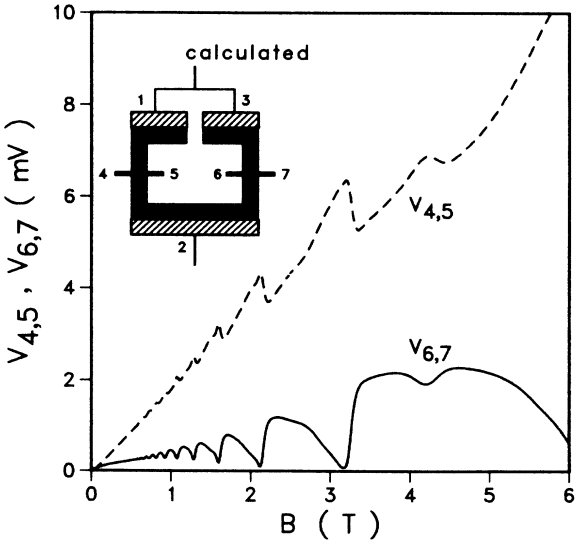

FIG. 13. Calculated Hall voltages for the "open square" geometry as given in an inset of Fig. 12(a). The asymmetry between both Hall voltages that is observed in experiments, Fig. 12(a), results from these calculations. The calculations start with measured R_H and $R_\square$.

over the sample.

For the closed square geometry we calculate the voltage $V_{1,2}$ along both sides from

$$V_{1,2}=R_H[I_1+I_2\exp(-N_{\square_1}R_\square/R_H)]+2N_{\square_2}R_\square I_1$$
$$=R_H[I_1\exp(-N_{\square_2}R_\square/R_H)+I_2]+2N_{\square_2}R_\square I_2\ , \tag{24}$$

where I_1 flows in the left branch of the square and I_2 in the right branch. This leads to $I_1=I_2$ and gives

$$V_{4,5}=V_{6,7}=\tfrac{1}{2}R_H I_0\ . \tag{25}$$

This is a totally symmetric solution. The observed voltages are less symmetric, especially at magnetic field strengths where the plateaus of the quantized Hall effect occur. This can be explained by a slight inhomogeneity of the electron density over the sample. The effects are comparable to the ones observed in the ring-shaped geometry.[9]

VI. CONCLUDING REMARKS

In this paper we have studied the influence of the sample geometry and the metal contacts on the measured voltages in the quantized Hall regime. We have not concentrated on the exact potential distribution within one sample, but on the voltages that can be measured on the contacts at the boundaries of the (sometimes multiply connected) samples. To interpret our experiments we have performed calculations using a homogeneous description that can be thought to originate from an adequate averaging over the inhomogeneous local resistivity tensor. This is meaningful when the sample has no large-scale inhomogeneities like gradients, or large regions with different mean electron densities. For this reason we used GaAs-$Al_xGa_{1-x}As$ heterostructures of good homogeneity and used symmetry considerations to verify that the measured effects are not due to deviations from the intended geometries. Our homogeneous description leads to questionable results for the geometries where the current distribution over parts of the sample is determined by the magnetoresistivity only. Experiments and calculations for a ring-shaped geometry, taking into account the measured inhomogeneity of the sample, are described earlier.[12]

The influence of large contacts on the measured voltages, even in the normal Hall bar geometry, can be very important for high-precision experiments at nonzero temperature. The measured Hall voltage can be smaller than the true Hall voltage. The dip in Hall resistance often observed at the high-magnetic field side of a Hall plateau can also be explained by the influence of the contacts. The measured two-terminal resistance can be much smaller than the Hall resistivity in geometries with large current contacts.

All our experimental results on special geometry samples can be explained by simply describing the sample by appropriately connected homogeneous rectangular semiconductor sections, some of them with metal contacts and each of them with its own local resistivity tensor. The current is distributed over these sections in accordance with Kirchhoff's laws. The Hall voltages are built up in the corners of current-carrying contacts. The effects at metal-semiconductor interfaces are taken into account. With the use of our model for the quantized Hall effect we have calculated the voltages that can be measured on the contacts of two multiply connected Hall bars. The calculations are in good agreement with the experiments. Even in the complicated geometries with large contacts we calculate voltages by splitting the geometry in simple parts, some of them with contacts, and describing the current transport in each part by a resistance per square and by a Hall resistance. The good agreement with experiments lends further support to the usefulness of a description of the quantized Hall effect as an effect that originates from a local resistivity tensor.[9] We do not take into account the existence of macroscopic quantum states or localization in this local resistivity tensor. The only quantum mechanics we use is the quantization of the density of states in a magnetic field, leading to vanishing magnetoresistivity in regions with an integer the filling factor. In inhomogeneous samples this resistivity has a spatial dependence that determines the distribution of the current over the sample. This spatial distribution (in real samples in combination with localization) makes that the Hall plateaus are quantized at the well-known values.

ACKNOWLEDGMENTS

It is a pleasure to thank C. E. Timmering for the skillful preparation of the samples. We are grateful to J. A. Pals and J. M. Lagemaat for valuable discussions.

[1]F. F. Fang, and P. J. Stiles, Phys. Rev. B **29**, 3749 (1984).
[2]D. A. Syphers, and P. J. Stiles, Phys. Rev. B **32**, 6620 (1985).
[3]W. van der Wel, J. E. Mooij, and C. J. P. M. Harmans, J. Phys. C **21**, L171 (1988).
[4]E. L. Al'tshuler, and N.N. Trunov, Meas. Techn. 29 796 (1986).
[5]Q. Niu and D. J. Thouless, Phys. Rev. B **35**, 2188 (1987).
[6]B. Neudecker and K. H. Hoffmann, Solid State Commun. **62**, 135 (1987).
[7]G. L. J. A. Rikken, J. A. M. M. van Haaren, W. van der Wel, A. P. van Gelder, H. van Kempen, P. Wyder, J. P. André, K. Ploog, and G. Weimann, Phys. Rev. B **37**, 6181 (1988).
[8]R. Woltjer, R. Eppenga, and M. F. H. Schuurmans, in *High Magnetic Fields in Semiconductor Physics,* edited by G. Landwehr (Springer-Verlag, Berlin, 1987), p. 104.
[9]R. Woltjer, Semicond. Sci. Tech. (to be published).
[10]A. C. Beer, *Galvanomagnetic effects in Semiconductors,* Vol. 4, of *Solid State Physics,* edited by H. Ehrenrecih, F. Seitz, and D. Turnbull (Academic, New York, 1963).
[11]M. E. Cage B. F. Field, R. F. Dziuba, S. M. Girvin, A. C. Gossard, and D. C. Tsui, Phys. Rev. B **30**, 2286 (1984).
[12]R. Woltjer, R. Eppenga, J. Mooren, C. E. Timmering, and J. P. André, Europhys. Lett. **2**, 149 (1986).